

DIRECT OBSERVATION OF THE FATE OF OCEANIC CARBON DIOXIDE RELEASE AT 800M

Edward T. Peltzer, Peter G. Brewer,
Gernot Friederich and Gregor Rehder
Monterey Bay Aquarium Research Institute
Moss Landing, CA 95039

Keywords: bubbles, carbon dioxide, clathrate hydrate, ocean sequestration

ABSTRACT

The rise rate and dissolution rate of freely released CO₂ in the ocean were measured to provide fundamental data regarding carbon sequestration in the upper ocean. These experimental observations were accomplished using MBARIs advanced remotely operated vehicle (ROV) technology. Small amounts of liquid CO₂ were released at 800 m depth and ambient temperature (4.4°C). The rising droplets were contained within an open ended acrylic chamber and were imaged with an HDTV camera. The mean rise rate for a droplet of initially 1 cm diameter observed over a one hour period was 12.4 cm/sec. The rise rate was initially about 10 cm/sec and it gradually increased to about 15 cm/sec as the bubble rose. The mean dissolution rate was 3.7 μmol/cm²/sec. Visual contact of the rising droplets was maintained for up to 1 hour and over 400 m initially suggesting a slow dissolution rate and long bubble lifetimes. However, 90% of the mass loss occurred within 30 minutes and 200 m of the release point.

INTRODUCTION

Concern about the rising levels of atmospheric CO₂ and the continued use of fossil fuels to meet ever increasing energy demands lead to consideration of the disposal of fossil fuel CO₂ in the ocean as a means of ameliorating greenhouse gas induced climate change (1,2). While many models of this process have been formulated (3,4), and various laboratory simulations have been carried out (5), there have been few direct oceanic experiments reported. With the availability of advanced ROV technology at MBARI, it was thought possible to carry out a controlled release of liquid and gaseous CO₂ in the open ocean, and to observe the processes taking place. In earlier work (6) we reported on contained experiments involving CH₄ and CO₂ to form hydrates. Here we present an initial experiment addressing the more difficult problem of observing and accurately measuring the behavior of a rising stream of freely released liquid CO₂. We choose this approach in order to evaluate the effectiveness of intermediate depth releases when all the co-varying properties of salinity, temperature, and pressure are present, and to represent the fluid dynamics of a rising cloud of liquid CO₂ droplets in the ocean.

In order to properly evaluate whether it is wise to proceed with any ocean disposal option, an accurate description of the fate of CO₂ injected into ocean water is necessary. At shallow depths (above about 350 m, depending upon the local temperature gradient) CO₂ is a gas, and readily dissolves. Below this depth, we encounter the gas hydrate phase boundary where a shell of CO₂-hydrate may be generated (7,8) on the bubble/droplet surface. Such a hydrate skin or shell, could have profound consequences; both slowing the rate of dissolution, increasing bubble lifetimes and increasing the thickness of the layer where the bulk of the CO₂ dissolves. Below about 400 m depth, pure CO₂ will exist as a liquid. Due to the relatively high compressibility of liquid CO₂ in comparison to seawater, the density ratio will invert at high pressure such that below about 2800 m depth a gravitationally stable release can be achieved (9). Release of CO₂ at depths deeper than this, may promote rapid and massive solid hydrate formation, and may lead to long oceanic residence times and effective sequestration from the atmosphere. The potential cost and technical difficulty of this deep injection scenario suggests the need to evaluate alternate injection scenarios at shallower depths.

While laboratory studies of the CO₂ clathrate-hydrate phase boundary and the solid phase have both been successful, it is difficult for a laboratory study to simulate the behavior of freely released material in motion, in a complex physical regime. Thus, several mathematical models have been devised to simulate this process and differing conclusions were reached. Holder et al. (10) modeled the behavior of a rising CO₂ plume incorporating a constantly growing film of solid hydrate. With time, this film slows the rise rate since CO₂-hydrate is more dense than either seawater or liquid CO₂, and eventually causes the combined mass to sink. Herzog et al. (3) modeled the dissolution rate of liquid CO₂ between 500 and 2000 m without the hydrate effects. They concluded that if the initial droplet radius is less than 1 cm, then complete dissolution would occur within less than 200 m. Very complete sets of model calculations incorporating plume dynamics have been carried out (3,4,11), and yet no field data exist to compare these models against.

EXPERIMENTAL

The experiments were executed beginning at 800m depth in Monterey Bay, off the coast of central California, during October 12-13, 1999, using the ROV *Ventana*. The ROV was equipped with an HDTV camera to observe the CO₂ released and the video tape recorded from this camera provides a permanent record of the work. The system captures images with a specially modified Sony HDC-750 high-definition television camera which digitizes the picture data and formats it to the SMPTE 292M HDTV interface standard with 2:1 interlace. The resolution of the images is 1035 pixels vertically and 1920 pixels horizontally which is about five times the resolution of conventional video. The image data is recorded with a Panasonic HD2000 high-definition video tape recorder without any further transcoding steps.

An earlier attempt at observing the free release of CO₂ had shown that it was impossible to maintain a CO₂ droplet cloud that was free to move in all dimensions within the field of view. Effects of the vehicle motions, strong lateral forcing due to local currents, and the similarity of appearance of a droplet of liquid CO₂ to the ubiquitous gelatinous marine organisms, all combined to frustrate continuous observation. Therefore a simple imaging box (89 cm long, 25 cm deep, and with a transparent face 30 cm wide) was constructed. It was open to the ocean at top and bottom, and mounted directly in front of the camera. The purpose of this box was to restrain lateral motions, while permitting free upward motion of the droplet plume. A meter scale within the box provided dimensional control within the imaged field. Additionally, the opaque back of the box hid the visually distracting marine snow in the background. The liquid CO₂ injector was modified slightly from that described earlier (9), and used a piston assembly, operated by the vehicle hydraulic system, to deliver 128 mL of liquid per stroke through a 1/8-inch orifice mounted on the back of the imaging box. Smaller volumes were delivered with partial strokes. A CTD instrument mounted on the ROV provided depth, temperature and salinity information for the duration of the experiment. The experiment depth was chosen to match plans for a future large-scale release of CO₂ off the coast of Hawaii (12).

With the known dimensions of the bubble box, and the meter scale attached to the rear wall, we have numerical reference points with which to quantify the images of droplets during ascent. The time at which an image was recorded was logged on the same time base as the vehicle depth (pressure), temperature, etc. Frame grabs from the HDTV video tape provide a convenient means to measure droplet dimensions by comparison to the numerical scale.

At first glance, this experiment is disarmingly simple, however experience has shown that there is more here than meets the eye. It requires the precise piloting of a 3 ton vehicle, subject to oceanic forcing in 3 dimensions, while imaging a small cloud of droplets with millimeter precision for one hour over hundreds of meters of ascent. The successful completion of this experiment is a tribute to the skill of the ROV pilots and engineers.

RESULTS

Two CO₂ release experiments were carried out. In the first experiment, the droplets rose from 800 m to 625 m depth during the course of 21 minutes, at which time the droplet escaped from the bubble box. In a second release, a droplet was followed from 800 m to 340 m depth during a period of about 1 hour. The depth versus time curve for the second release is shown in Figure 1. Small errors in positioning the bubble in the vertical center of the box are assumed to be negligible when compared to the over 400 m rise of the experiment. The temperature profile recorded during this experiment is overlain on the relevant portion of the phase diagram for CO₂ in seawater in Figure 2. Note that visual contact with the bubble was lost just below the hydrate phase boundary. The nearness of this significant boundary attracted our attention initially, but the evidence suggests that the visual loss of the bubble at this point was coincidental.

A mean ascent rate of 12.8 cm/sec was observed during the first release and 12.4 cm/sec for the second, longer, experiment. Close inspection of the data revealed a measurable increase in velocity with decreasing pressure and concomitant diminishing droplet diameter. By fitting a second-order polynomial to the depth versus time data, we were able to better estimate (from the first derivative of this equation) that the rise rate was 10.2 cm/sec initially, increasing gradually to 14.9 cm/sec just before contact was lost with the bubble. A dramatic change in rise rate coincident with the transition from droplet to bubble on crossing the liquid-to-gas phase boundary, was not observed. While the data can be smoothly fit with a second order polynomial (see Figure 1) with no evidence of a discontinuity at that point, data above this phase boundary are sparse. As the droplets rose, they shrink from dissolution, expand from pressure release, and encounter progressively warmer and less dense seawater. The net result of this complex process is the small and relatively simple to model increase in rise rate versus time that was observed.

The ideal experiment of a single purely spherical droplet proved unrealistic. Early we observed that bubble collisions were frequent, and that rafts of CO₂ droplets remained strongly attached to

each other and that these rafts persisted for very long periods. At the same time, one could recognize a distinctively shaped unit and follow it within the droplet cloud. One such unit was found which later formed a droplet pair. The changing dimensions of this droplet pair during their ascent are given in Table 1. These complex shapes, rotating in three dimensions present varying aspect ratios to the camera and frame grabs were carefully selected to remove this effect.

Occasionally, droplets collided with and stuck to the walls of the bubble box. It was possible to free the droplet with a sudden lateral ROV motion, but the possibility of mass loss to the walls, rather than by dissolution remains. Furthermore, boundary flow occurs along the walls of the bubble box as the vehicle rose, and droplets were consistently drawn to this region. In spite of these difficulties it proved possible to maintain the droplets in free flow for the greater part of the ascent suggesting that any bias due to boundary effects is small. Images, from an alternate experiment, where droplets of liquid CO₂ were allowed to rise freely while the ROV was held stationary and thus no boundary flow effects are present, are being analyzed to determine the extent of the impact of the boundary flow upon the measured rise rates.

Table 1 presents the data on droplet size versus depth. Additionally, these data are plotted versus time in Figure 3. From these observations, and literature values on the density of liquid CO₂ as a function of pressure and temperature, it is possible to calculate the mass loss with time. These results show that droplet diameter changes as a linear function of time, and gives a dissolution rate for liquid CO₂ of 3.7 $\mu\text{mol}/\text{cm}^2/\text{sec}$. This result compares well with the results of Aya et al. (5) from laboratory pressure vessel studies at 30 MPa and 4.5°C. The laboratory measurements yield a value of 1.7 or 2.8 $\mu\text{mol}/\text{cm}^2/\text{sec}$ with and without a hydrate skin, respectively. The slightly higher rate obtained in the natural environment, may be due to the lower pressures involved and the complex physical situation, or the dynamics of a rising droplet stream (13,14).

In earlier work (6,9), we have demonstrated that within the phase boundary, CO₂ hydrate forms readily, almost instantaneously, on vigorous mixing of CO₂ and seawater. In these experiments, hydrate formation is usually recognizable by a change in optical reflectivity at interface of the phases, and by a white cloudy appearance. Based upon the imagery we obtained, it is not possible to state with certainty, whether the droplets followed here maintained a hydrate skin. Immediately after injection, the droplets appear to have a stiff surface skin, and droplet rafts formed and maintained a stick like shape. As the droplets rose they became more rounded, and soon appeared to be hydrate free. It is possible that some hydrate may have formed inside the release tube and was carried out with the droplets. However it is impossible, on the basis of these observations, to say whether the dissolution rate observed was affected by a molecular boundary layer of hydrate, or whether the relatively slow dissolution is simply the result of the high degree of immiscibility between liquid CO₂ and seawater.

The choice of a scenario for the long term sequestration of anthropogenic CO₂, either via a rising stream of CO₂, or via the formation of a sinking plume with hydrate formation (9) has yet to be made. The results presented here should allow a more accurate prediction of the CO₂/pH field, and the environmental effects, surrounding an injection point. However, a critical property for the longer term will be the effectiveness of the process in terms of sequestration. For example, the depths chosen here cover the 27.3 - 26.8 (σ_θ) isopycnal surfaces. While the 26.8 surface is the most dense seawater to outcrop seasonally at the surface in the North Pacific, Warner et al. (15) have recently mapped the ventilation age of this surface demonstrating that it was relatively recently (12-32 years) exposed to contact with the atmosphere. This probably represents the shallowest depth at which disposal in this ocean basin is likely to be effective as a sequestration option, although other shallow disposal scenarios have also been considered (13,14).

The small-scale ROV experiments described here are a "first effort" to evaluate these processes, and appear to offer an effective way to approach the problem without the costs and problems associated with larger-scale releases. We were not yet able with these small quantities to easily simulate some of the changes in local seawater density, and "peeling" of the plume predicted by large scale fluid dynamic modeling (11). At the same time, it should be recognized that the results reported here pertain to isolated bubbles moving in a more or less undisturbed ocean. Differences with the large-scale releases will no doubt be found. It is not only possible to extend these studies to include biological effects (16) but it is also desirable and this work is in progress.

ACKNOWLEDGEMENTS

The authors would like to thank the Captain and crew of the RV *Point Lobos*, and the pilots of the ROV *Ventana*. Without their skilled support, this research would not have been possible. This work was supported by a grant to MBARI from the David and Lucile Packard Foundation.

REFERENCES

1. C. Marchetti, *Climate Change* **1**, 59 (1977).
2. N. Handa and T. Ohsumi, *Direct Ocean Disposal of Carbon Dioxide* (Terra Scientific Publishing, Tokyo, 1995).
3. H. Herzog, D. Golomb, S. Zemba, *Envir. Prog.* **10**, 64 (1991).
4. H. Drange, P. Haugan, *Tech. Rep. 54, NERSC* (1992).
5. I. Aya, K. Yamane, H. Nariai, *Energy* **22**, 263 (1997).
6. P. G. Brewer, F. M. Orr, Jr., G. Friederich, K. A. Kvenvolden, D. L. Orange, *Energy Fuels* **12**, 183 (1998).
7. E. D. Sloan Jr., *Clathrate Hydrates of Natural Gases* (Dekker, New York, 1990).
8. W. J. North, V. R. Blackwell, J. J. Morgan, *Environ. Sci. Technol.* **32**, 676 (1998).
9. P. G. Brewer, G. Friederich, E. T. Peltzer, and F. M. Orr, Jr., *Science* **284**, 943 (1999).
10. G. D. Holder, A. V. Cugini, R. P. Warzinski, *Environ. Sci. Technol.* **28**, 276 (1995).
11. G. Alendal, H. Drange, *J. Geophys. Res.* In Press.
12. E. Adams, H. Herzog, *Tech. Rept., MIT* (1998).
13. P. Haugan, H. Drange, *Nature* **357**, 318 (1992).
14. R. Clift, J. R. Grace, M. E. Weber, *Bubbles, Drops and Particles* (Academic Press, New York, 1978).
15. M. J. Warner, J. L. Bullister, D. P. Wisegarver, R. H. Gammon, R. F. Weiss, *J. Geophys. Res.* **101**, 20,525 (1996).
16. M. N. Tamburri, E. T. Peltzer, G. E. Friederich, I. Aya, K. Yamane, P. G. Brewer, *Mar. Chem.*, In Press.

Table 1

Measured Liquid CO₂ Droplet Characteristics during Ascent from 800m Depth

Elapsed Time (min)	Depth (m)	Temp. (°C)	Droplet Diameter (cm)		CO ₂ Density (g/cc)	Amount of CO ₂ (millimoles)		Rise Rate (cm/s)
			(a)	(b)		(a)	(b)	
0	804.5	4.398	1.10		0.9423	14.92		10.2
14.23	706.3	4.740	0.75		0.9310	4.67		11.3
23.13	649.1	4.994	0.60	1.10	0.9235	2.37	14.63	12.0
29.82	602.1	5.165	0.45	0.90	0.9171	0.99	7.96	12.5
43.08	496.8	5.449	0.20	0.80	0.9021	0.09	5.50	13.5
49.73	447.3	5.995		0.45	0.8910		0.97	14.0
61.65	341.2	7.291		0.25	0.8632		0.16	14.9

The initial droplet tracked (a) was joined at about 650 m depth by a second, larger, bubble (b) which became attached. No change in rise rate could be detected due to the attachment, and the changing size of each droplet could be independently determined. The mean density of liquid CO₂ during the rise of the droplets was 0.92 (a) and 0.90 (b), respectively. Thus, a 1 cm³ droplet contains 21.1 (a) or 20.4 (b) millimoles CO₂. We calculate the dissolution rate (Γ) from the slope of:

$$(r_t - r_0) = -V_m \times \Gamma \times (t - t_0), \quad [1]$$

where V_m is the specific volume (mmol/cm³), r_0 and r_t are initial droplet radius and droplet radius at time t , and t_0 and t are initial time and the time elapsed since t_0 . The observed dissolution rate was 3.7 $\mu\text{mol}/\text{cm}^2/\text{sec}$.

The rise rate was determined by fitting a second-order polynomial to depth versus time to obtain:

$$Z_t = -2.250 \times 10^{-2} \times t^2 - 6.145 \times t + 799.2, \quad [2]$$

then taking the first derivative of equation [2] to yield the rise rate at time, t :

$$R_t = -0.0450 \times t - 6.145. \quad [3]$$

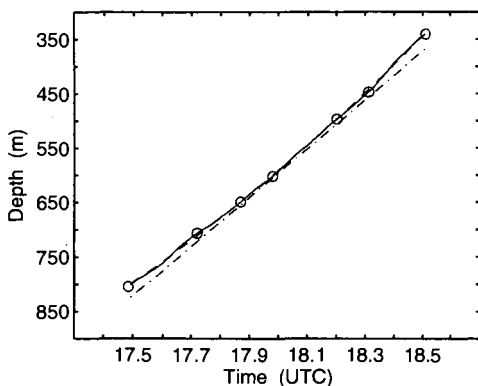


Figure 1. Plot of the observed ROV depth vs time for the second CO₂ release (solid line) and selected droplets (o). The mean rise rate for this release is shown as the dot-dash line tangent to the mid-point of the data curve. The dashed line is the second order polynomial fit to depth.

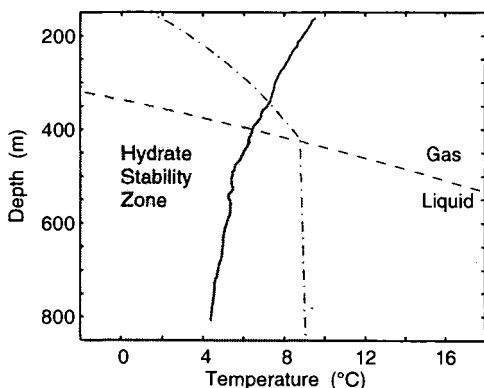


Figure 2. The observed ocean temperature profile recorded during the droplet rise experiments, overlaid on the CO₂ phase diagram for seawater. While the injection point is far inside the region for hydrate formation, the droplet crossed the liquid-to-gas phase boundary at about 400 m depth, and visual contact with the droplet was lost at about 340 m depth.

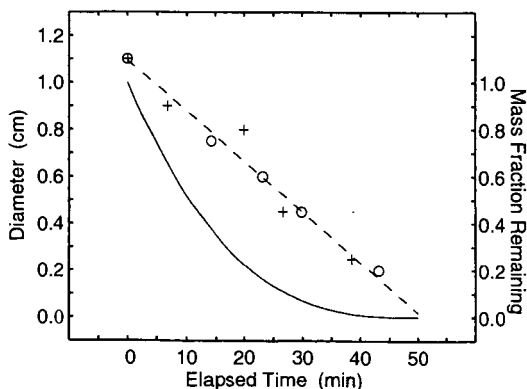


Figure 3. Plot of the changing droplet diameter with time, and remaining mass fraction of the droplets. The droplet size derived from HDTV video analysis, as listed in Table 1, is shown by circles (a) and crosses (b), respectively. The dashed line indicates the trend of diameter versus time calculated from equation (1) with a dissolution rate of $3.7 \mu\text{mol}/\text{cm}^2/\text{sec}$. The solid line shows the calculated remaining mass fraction relative to the initial mass of the CO₂ droplets.